

Green-Emitting Poly[(2-alkoxy-5-methyl-1,3-phenylenevinylene)-*alt*-(1,4-phenylenevinylene)s]: Effect of Substitution Patterns on the Optical Properties

Liang Liao and Yi Pang*

Department of Chemistry & Center for High Performance Polymers and Composites, Clark Atlanta University, Atlanta, Georgia 30314

Liming Ding and Frank E. Karasz

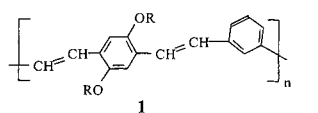
Department of Polymer Science and Engineering, University of Massachusetts, Amherst, Massachusetts 01003

Received December 17, 2001; Revised Manuscript Received February 21, 2002

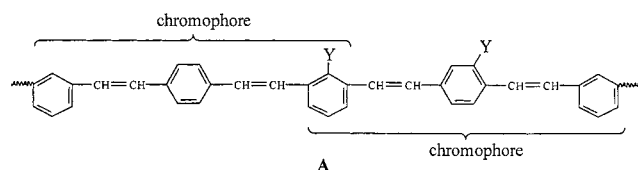
ABSTRACT: Green-emitting poly[(2-alkoxy-5-methyl-1,3-phenylenevinylene)-*alt*-(1,4-phenylenevinylene)]s (**2**) were synthesized via the Wittig–Horner reaction. The polymers were yellow resins with the molecular weights as high as 54 600. On the basis of FT-IR and ¹H NMR spectra, the olefins in the polymers were confirmed to be predominantly in the *trans* configuration. UV–vis absorption of **2** ($\lambda_{\text{max}} \approx 374 - 377$ nm) was about 20 nm blue-shifted from that of poly[(1,3-phenylenevinylene)-*alt*-(2,5-dialkoxy-1,4-phenylenevinylene)]s (**1**), although the chromophores in the former had the same number of alkoxy substituents as in the latter. Comparison of **2** with the model compound **7** showed that the shorter conjugation length observed from **2** (relative to **1**) was the intrinsic property of the chromophore. Polymer **2** also exhibited a higher photoluminescence (PL) than **1** in both solution and film states, indicating the effect of the substitution pattern on the optical properties of the polymers. The vibronic structures were assigned with the aids of the low-temperature UV–vis and fluorescence spectroscopy. LED devices using **2** gave green EL output (emission λ_{max} at 496 and 520 nm) with the external quantum efficiency of 0.082%.

Introduction

Since the discovery of polymeric light-emitting diodes (LEDs)¹ in 1990, π -conjugated polymers have attracted increasing attention over the past decade² because of their potential applications in display technologies. The unique combination of their structural, mechanical, photonic, and electronic properties also renders them attractive candidates for use as plastic lasers³ and chemical sensors⁴ and for use in other fields.⁵ Recent studies⁶ have shown that poly[(*m*-phenylenevinylene)-*alt*-(*p*-phenylenevinylene)] (PmPVpPV) derivatives (**1**)



(a: R= n-Butyl; b: R= n-Hexyl; c: R= n-Octyl)



are green-emitting with high PL efficiency. While the *p*-phenylene and *m*-phenylene are alternately placed along the polymer chain, the side chain substituents in **1** are only present on the *p*-phenylene unit. It is known that different substitution patterns⁷ on the π -conjugated polymers could significantly influence their luminescent properties. It would be interesting to examine whether the substitution on a different type of phenylene unit will affect the luminescent properties of the PmPVpPV

derivative **2**, in which the substituents are only present on the *m*-phenylene unit.

The molecular fragment **A** represents a section of chain structure in PmPVpPV. As demonstrated in our previous report,^{6a} the chromophore of the polymer can be described as *p*-phenylenedivynylene sandwiched between the two adjacent *m*-phenylene units. A unique feature in PmPVpPV is that the *m*-phenylene is shared between the two adjacent chromophores. A substituent “Y” placed on an *m*-phenylene is, therefore, expected to influence the two adjacent chromophores simultaneously, while that on a *p*-phenylene is expected to influence only one chromophore. In other words, substitution on a different type of the phenyl rings (*m*-phenylene or *p*-phenylene) along the PmPVpPV backbone would perturb the electronic band structure of the polymer in different fashion. The fact that the *m*-phenylene occurs at the end of the chromophore may also contribute to a different substituent effect in comparison with the *p*-phenylene at the center of the chromophore. Although previous studies⁶ have been focused on attachment of the substituent to the *p*-phenylene unit as shown in **1**, no report has been found in the literature to put substituent on the *m*-phenylene of PmPVpPV. Availability of *m*-phenylene-substituted PmPVpPVs will allow one to evaluate the substitution effect, and to establish the valuable structure–property correlations, which are desirable for future material development. Here we report the synthesis and characterization of **2**, along with its optical properties.

Results and Discussion

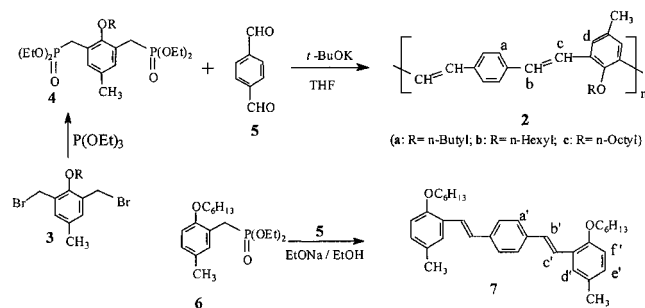
Polymer **2** was synthesized as shown below by using the Wittig–Horner reaction,⁸ which is known to produce *trans*-alkenes. In the polymer **2**, the *p*-phenylene and

Table 1. Spectroscopic Data for Polymers **2** and the Model Compound **7**

polymer	content ^a of <i>trans</i> -CH=CH (%)	<i>M_w</i> (PDI)	DP	emission ^b λ_{\max} (nm)	UV-vis abs ^b λ_{\max} (nm)	ϕ_{PL}
2a	85	54600 (1.8)	104	412, 436, 464	377	0.72
2b	86	22000 (1.8)	38	412, 436, 465	377	0.71
2c	88	6820 (1.2)	16	412, 436	374	0.72
7	93			413, 436, 464 (sh)	371	0.88

^a The content of *trans*-CH=CH was estimated from the ¹H NMR spectra in CDCl₃ solvent. ^b The absorption and emission spectra were acquired from their respective THF solutions at 25 °C.

m-phenylene units were alternated along the backbone, thereby producing a chromophore with a uniformly defined structure. The polymers were yellow resins with the molecular weight as high as 54 600 (Table 1). The number-average degrees of polymerization of **2** were determined to be $n \approx 104$, 38, and 16 for **2a**, **2b**, and **2c**, respectively. Polymer **2** exhibited good solubility in common organic solvents such as THF, chloroform, and toluene. It appeared that only a short alkyl side chain on the substituted phenyl rings was necessary to keep the polymer soluble. Uniform thin films could be cast from the polymer solutions. To aid the polymer structure characterization, the model compound **7** was synthesized similarly by reacting **6** with benzene-1,4-dicarbaldehyde **5**.



The high intensity of absorption at $\sim 965 \text{ cm}^{-1}$ in the IR spectrum of **2** (Figure 1) indicated that the olefin groups in the polymer were predominantly in the *trans* configuration.⁹ The olefinic and aromatic region of the ¹H NMR spectrum of **2** is shown in Figure 2, where the resonance signals were assigned by using the same labels as in the structures **2** to indicate the corresponding aromatic and olefinic protons. The presence of the doublet signals at about 7.13 and 7.47 ppm (marked “b” and “c” in Figure 2) with a large coupling constant ($J = 16.4 \text{ Hz}$) confirmed the *trans* stereochemistry of

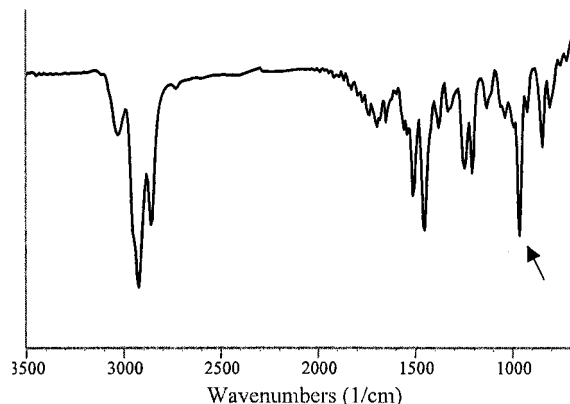


Figure 1. Infrared spectrum of **2b** film on NaCl plate. The vertical scale is transmittance in arbitrary units. The arrow marks the absorption for olefinic C–H out-of-plane deformation (*trans*-CH=CH at $\sim 965 \text{ cm}^{-1}$).

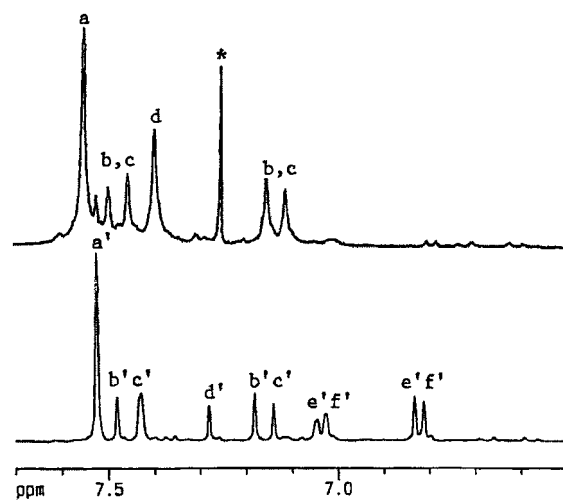


Figure 2. ¹H NMR of **2b** (top) and **7** (bottom) (only aromatic and olefinic region is shown for clarity). The starred signal at 7.25 ppm is attributed to trace CHCl₃.

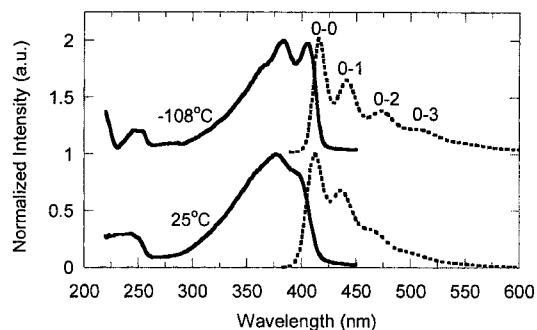
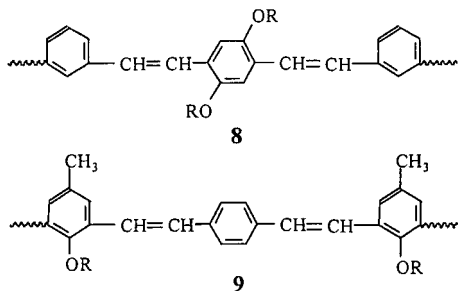


Figure 3. UV-vis (solid line) and PL (dotted line) spectra of polymer **2b** in THF solution at +25 and $-108 \text{ }^\circ\text{C}$. The spectra at $-108 \text{ }^\circ\text{C}$ are offset from those at $25 \text{ }^\circ\text{C}$ for clarity.

CH–CH in the polymer.¹⁰ The assignment of the resonance signals in the ¹H NMR spectrum of the polymer was further supported by the observed same coupling pattern (*trans*-CH=CH) from the model compound **7**. The relative signal intensity between the singlet at $\sim 7.39 \text{ ppm}$ (proton “d”) and the doublet at ~ 7.13 and 7.49 ppm concluded that the majority of olefins in the polymer was in the *trans* configuration. The content of *trans*-CH=CH bond linkage (Table 1) was estimated by integrating the proton resonance signals of $-\text{OCH}_2-$ unit in the alkoxy side chains, which were shown to be sensitive to the nearby *cis*-CH=CH or *trans*-CH=CH configuration^{6a} in *m*-phenylene-containing PPVs.

Photoabsorption and Photoluminescence (PL). The UV-vis spectra of the polymer **2** in dilute THF solution (Figure 3) showed one major band with absorption λ_{\max} at about 377 nm, which is quite different from that of **1** exhibiting two absorption bands^{6a} at about 326 and 397 nm. It appears that the substitution patterns do have some effect on the electronic band structure of

the chromophores. Resulting from the *m*-phenylene interruption, the conjugation length of the chromophore in **1** and **2** would be determined by the fragments **8** and **9**, respectively. While both fragments **8** and **9** contain



the same number of alkoxy groups, the presence of two methyl groups in the latter are expected to cause further increase in conjugation length (additional bathochromic shift).¹¹ On the contrary, the observed conjugation length for **2** ($\lambda_{\max} = 377$ nm) is about ~ 20 nm blue-shifted from the absorption λ_{\max} of polymer **1** (~ 397 nm).^{6a} This notable difference in conjugation length between **1** and **2** was also observed in their emission spectra (Figure 3), where the emission λ_{\max} of the highest energy band was at 412 and 444 nm for **2** and **1**, respectively. The fluorescence quantum efficiency¹² of **2** was estimated to be $\phi_{\text{fl}} \approx 0.71$, in comparison with that of **1** ($\phi_{\text{fl}} \approx 0.66$).

To gain further understanding on the nature of the electronic structure of the material, spectroscopic comparison was made between polymer **2** and its model compound **7**. As shown from Figures 3 and 4, solution of **7** in THF exhibits absorption and emission profiles very similar to those of **2**. The small difference between the λ_{\max} values of **2** and **7** (~ 6 nm in UV-vis absorption, and ~ 1 nm in emission) (Table 1) is within the range of the anticipated substituent effect, indicating an effective conjugation interruption at *m*-phenylene. Very similar conjugation lengths displayed from **2** and **7** strongly suggests that the shorter conjugation length observed from **2** (relative to **1**) is the intrinsic property of the chromophore fragment **9**. Because of the different substitution pattern, the steric interaction between the side chains and π -conjugated polymer backbone in polymer **2** is expected to be different from that in polymer **1**. This difference in steric interaction, however, may not be sufficient to cause a significant change in the conjugation length of the polymer chromophores.

Simple comparison between polymers **2** and **1** shows that the number of alkoxy group per repeating unit in **2** is only half of that in **1**. This might not be the major reason to account for the short conjugation length of **2**, as it is in contrary to the observation that both **2b** and **7** exhibit very similar conjugation length. The different arrangement of the substituent (or substitution pattern), therefore, might play an important role in the observed shorter conjugation length from **2**. As seen from their respective chromophores, the alkoxy substituents in **9** appears at the end of the chromophore in comparison with that in **8** at the center of the chromophore. Comparison of the UV-vis absorption λ_{\max} values between the chromophore model compounds for **2** and **1** offers further support to the substitution effect, as **7** is blue-shifted ($\Delta\lambda_{\max} \approx 17$ nm) from 1,4-bis(2'-phenylethenyl)-2,5-dihexyloxybenzene¹³ to a very similar degree. The observed blue-shift from polymers **1** to

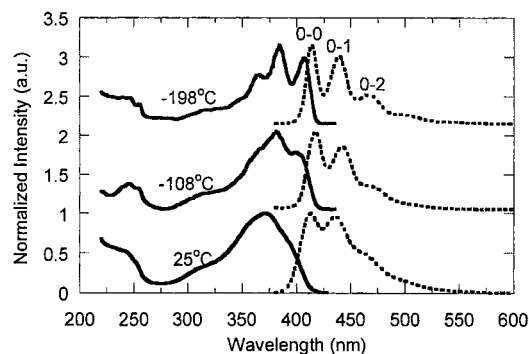


Figure 4. UV-vis (solid line) and PL (dotted line) spectra of **7** at +25 and -108 °C in THF, and at -198 °C in a solvent mixture (diethyl ether, ethanol, and 2-methylbutane in a ratio of 1:1:1). The spectra at different temperature are offset for clarity.

2 suggests that some minor tune in the electronic band-gap of PmPVpPV can be achieved by simply placing substitution on *m*- or *p*-phenylene units.

Low-Temperature UV-Vis and PL. The solution UV-vis spectrum of **2** at 25 °C (Figure 3) showed a major peak at 377 nm, and a shoulder at ~ 395 nm. As the temperature was lowered to -108 °C (still in the liquid state), the shoulder was resolved into a pronounced peak due to the reduced rotation and increased viscosity at the low temperature. In addition, the spectrum was slightly red-shifted (~ 6 nm) with the absorption λ_{\max} values at 383 and 406 nm at the low temperature. The fluorescence spectrum at -108 °C also became more resolved, showing more transitions with the emission λ_{\max} at 416, 441, and 473 nm (corresponding to the wavenumber of 24 038, 22 676, and 21 142 cm^{-1} , respectively). The vibrational energy levels of **2** in the ground state (as shown from the emission peaks) appears to be about equally spaced with a wavenumber separation of about 1362 cm^{-1} , or a wavenumber separation of about 25 nm. The energy difference between the overlapping low-energy absorption band ($\lambda_{\max} = 406$ nm) and the high-energy emission band ($\lambda_{\max} = 416$ nm) is estimated to be about 593 cm^{-1} , which is significantly smaller than the required adjacent vibrational energy gap of at least 1362 cm^{-1} for a lower energy level in an anharmonic oscillator model.¹⁴ Therefore, it is likely that the emission bands at 416, 441, and 473 nm in the low-temperature fluorescence spectrum of **2** are corresponding to 0-0, 0-1, and 0-2 transitions, respectively. The fluorescence spectra of the polymers (Figure 3) also revealed a characteristic pattern, in which the short-wavelength vibrational band (0-0 transition) was the most intense emission, and the intensity of the emission bands gradually decreased with increasing wavelength. This characteristics suggested that the geometry of the chromophore in the excited state was very similar to that of its ground state, based on the Franck-Condon principle.¹⁵

The solution UV-vis spectrum of the model compound **7** at 25 °C showed a major absorption band ($\lambda_{\max} = 371$ nm). As the temperature was lowered to -108 °C, a new band at 400 nm became partially resolved in addition to the major absorption band at 380 nm. To further confirm the presence of the new band at 400 nm, the sample **7** in a solvent mixture¹⁶ of diethyl ether, ethanol, and 2-methylbutane was cooled to -198 °C in liquid nitrogen to form a clear transparent glass. The absorption spectrum at -198 °C (shown in Figure 4)

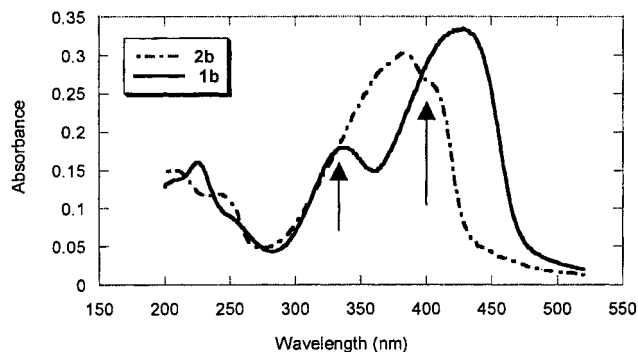


Figure 5. UV-vis absorbance of films **1b** and **2b**. The arrows mark the wavelength at 332 and 397 nm, respectively.

exhibited clearly resolved bands with absorption $\lambda_{\max} = 366, 384,$ and 406 nm. The fluorescence spectrum of **7** at the low temperature also became more resolved. By using the same reasoning for assigning the vibronic structure of polymer **2**, the emission bands at $414, 439,$ and 466 nm in the spectrum of **7** at -198 °C were assigned to $0-0, 0-1,$ and $0-2$ transitions, respectively. By using the $0-0$ and $0-1$ bands at 417 nm ($23\,981$ cm^{-1}) and 442 nm ($22\,624$ cm^{-1}) from the fluorescence spectrum of **7** at -108 °C, the vibrational energy gap of **7** in the ground state was estimated to be ~ 1357 cm^{-1} , which is comparable to that of ~ 1362 cm^{-1} for **2**. The vibronic structures of **7** revealed from the low temperature absorption and emission spectra are remarkably similar to that of **2**, further confirming the assumption that the electronic band structure of the polymer is determined by the fragment **9**. It should be pointed out that the vibrational energy gap of **2** (~ 1362 cm^{-1}) is noticeably larger than that of **1** (~ 1300 cm^{-1}),¹⁷ which seems in agreement with the slightly higher PL efficiency of the former.

Thin-Film Optical Properties. To further examine the optical properties in the solid state, polymer films were prepared by spin-casting the polymer solution (2 mg/mL in THF) on a quartz plate at a spin rate of about 1700–1800 rpm. The films **1** and **2** thus prepared were uniform and had very similar thickness as shown by their similar absorbance at absorption λ_{\max} (Figure 5). Polymer **2** exhibited one major absorption band at 383 nm, in comparison with two absorption bands at about 336 and 425 nm observed from the film **1**. In addition, the absorption profile of **2** in the solid state is quite similar to that in solution, supporting the assumption that the chromophore in the polymer is well-defined. While the UV-vis spectra of both films **2** and **1** were slightly red-shifted from their respective spectra in THF solutions ($\lambda_{\max} = 377$ for **2**, and $\lambda_{\max} = 410$ for **1**), the peak absorption difference $\Delta\lambda_{\max}$ between the film and solution spectra is estimated to be ~ 6 nm for **2** and ~ 15 nm for **1**. The observed smaller bathochromic shift from solution to film states indicates that the chromophore in **2** seems to be less affected by the molecular environments than that of **1**.

Excitation spectra under the identical conditions indicated that emission intensity of film **2** in general was stronger than that of **1** (Figure 6), when the excitation wavelength is between 275 and 420 nm. Although the excitation spectra of **1** and **2** exhibited the similar profile as observed in their respective absorption spectra, the excitation λ_{\max} values are noticeably different from the respective absorption λ_{\max} values. The emission spectra were acquired while the films were

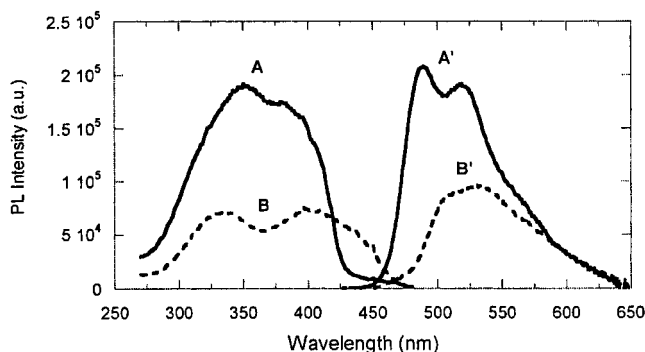


Figure 6. Curves A and B are excitation spectra for films **2b** and **1b** while monitoring at 500 nm. Curve A' and B' are respective emission spectra while the films were excited at 397 nm. The emission peaks for **2b** (in curve A') are at 490 and 518 nm and that for **1b** is at 530 nm.

excited at 397 nm, where both films under study had the same absorbance (Figure 5). The same emission profiles were also observed when the films were excited at 332 nm. The relative emission intensity, as determined by the ratio of integration peak area of **2** to **1**, was estimated to be about 1.8 and 1.9 when excited at 397 and 332 nm, respectively. Therefore, the substitution pattern on the polymer backbone appears to have significant influence on the optical properties of the materials, including the electronic band structure and luminescent efficiency. Emission of film **2** showed two distinctive peaks at 490 nm ($20\,408$ cm^{-1}) and 518 nm ($19\,305$ cm^{-1}).

EL Properties. LED devices ITO/PEDOT/polymer/Ca were fabricated to examine the EL properties. The device from polymer **2b** gave green emission at 496 and 520 nm (Figure 7) in comparison with that from **1** at 513 and 539 nm.^{6a} The EL spectrum of **2b** matched very well with its PL spectrum, indicating that both PL and EL originated from the same radiative decay process of the singlet exciton.¹⁸ Turn-on voltage for the device of **2b** was ~ 4.5 V (Figure 7). The external quantum efficiency of the device was estimated to be 0.082% for **2b**.

Experimental Section

Materials and Instrumentation. Terephthalaldehyde (99%), triethyl phosphite $\text{P}(\text{OEt})_3$, 4-hydroxytoluene (Acros Organics), potassium *tert*-butoxide (1.0 M in THF), and hydrogen bromide (30 wt % solution in acetic acid) (Aldrich Chemical Co.) were used without further purification. Solvents were dried, distilled, and stored under nitrogen or argon. Polymer **1b** was synthesized by using the Wittig–Horner reaction,^{6d} and 1-alkoxy-2,6-bis(bromomethyl)-4-methylbenzene **3** was prepared by using the procedure reported previously.¹⁹ IR spectra were recorded on a Nicolet Impact 400 FT-IR spectrometer from films on NaCl plates. UV-vis spectra were recorded either in distilled dry tetrahydrofuran (THF) or from films spin-cast on quartz plates on a Hewlett-Packard 8543 diode array spectrophotometer. ¹H NMR spectra were acquired on a Bruker ARX400 spectrometer. Fluorescence spectra were recorded on a PTI steady-state fluorometer at 23 ± 1 °C. Corrected fluorescence spectra of the polymer films were recorded on quartz plates in air. The solution PL quantum yields (ϕ_f) were measured relative to quinine sulfate in 0.5 M H_2SO_4 at 25 °C, by using the same procedure^{6a} as described previously. Size exclusion chromatography (SEC) was carried out on a Viscotek SEC assembly consisting of a model P1000 pump, a model T60 dual detectors, a model LR40 laser refractometer, and three mixed bed columns (10 μm). Polymer concentrations for SEC experiments were prepared in a concentration of about 3 mg/mL. The SEC system was

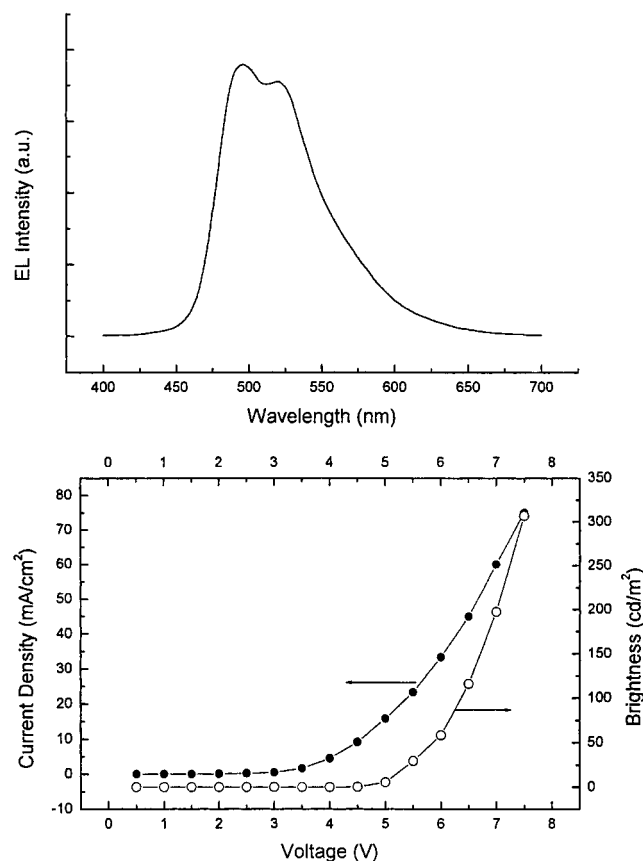


Figure 7. EL spectrum (top) and current density–voltage–brightness relationship (bottom) for the device ITO/PEDOT/2b/Ca.

calibrated by using narrow and broad polystyrene standards prior to use. The polystyrene standards were purchased from American Polymer Standards Corp.

Synthesis of Poly[(2-hexyloxy-5-methyl-1,3-phenylenevinylene)-*alt*-(1,4-phenylenevinylene)] (2b). A mixture of 2,6-bis(bromomethyl)-1-hexyloxy-4-methylbenzene **3a** (0.567 g, 1.50 mmol) and triethyl phosphite (0.548 g, 3.30 mmol) was heated at 155–165 °C under an argon atmosphere for 2 h. The excess triethyl phosphite and byproducts were removed under vacuum (0.5 mmHg, 100 °C for 0.5 h). The obtained 4-alkoxy-1-methyl-3,5-xylene tetraethyldiphosphate (**4**)¹⁸ (a colorless liquid) was dissolved in anhydrous THF (25 mL) with terephthalaldehyde (**5**) (0.201 g, 1.50 mmol). To this solution was added dropwise potassium *tert*-butoxide (1 M in THF, 3.0 mL) at room temperature via a syringe over a period of 15 min. A red-purple color was formed and quickly disappeared upon the addition of potassium *tert*-butoxide solution. After addition, the solution was stirred for an additional 3 h at room temperature. The resulting solution was separated from the salt, and the polymer was precipitated out via dropwise addition to methanol (125 mL). The yellow precipitate was collected and washed with methanol on a Soxhlet extractor for 48 h, and dried by vacuum to afford a light yellow resin (0.150 g, yield 30.7%), which had the following spectral properties. ¹H NMR (400 MHz, CDCl₃), δ : 0.82–0.95 (br, 3H, $-\text{CH}_2\text{CH}_3$), 1.36–1.44 (br, 4H, $-\text{CH}_2-$), 1.51–1.64 (br, 2H, $-\text{CH}_2-$), 1.81–1.92 (m, 2H, $-\text{CH}_2-$), 2.38 (s, 3H, Ar- CH_3), 3.83 (br, 1.68H, $-\text{OCH}_2-$ (in *trans*-olefin fragment)), 3.88 (br, 0.32H, $-\text{OCH}_2-$ (in *cis*-olefin fragment)), 7.13 (d, $J = 16.4$ Hz, 2H, *trans*-CH=CH-), 7.40 (s, 2H, Ar-H), 7.47 (d, $J = 16.4$ Hz, 2H, *trans*-CH=CH-), 7.45 (s, 4H, Ar-H). IR (NaCl, thin film), ν_{max} (cm⁻¹): 3033 (w), 2925 (s), 2863 (s), 1513 (m), 1451 (s), 1382 (w), 1250 (w), 1212 (m), 965 (s), 865 (w). Anal. Calcd for C₂₃H₂₆O: C, 86.75; H, 8.23. Found: C, 86.08; H, 8.29.

Poly[(1-butoxy-4-methyl-2,5-phenylenevinylene)-*alt*-(1,4-phenylenevinylene)] (2a) was synthesized in 75% yield

by using the same procedure as for **2b**. ¹H NMR (400 MHz, CDCl₃), δ : 1.04 (br, 3H, $-\text{CH}_3$), 1.68 (br, 2H, $-\text{CH}_2-$), 1.89 (m, 2H, $-\text{CH}_2-$), 2.24 (s, 0.47H, Ar- CH_3 (*cis*-olefin fragment)), 2.43 (s, 2.53H, Ar- CH_3 (*trans*-olefin fragment)), 3.88 (m, 1.69H, $-\text{OCH}_2-$ (*trans*-olefin fragment)), 3.97 (m, 0.31H, $-\text{OCH}_2-$ (*cis*-olefin fragment)), 7.17 (d, $J = 16.4$ Hz, 2H, *trans*-CH=CH-), 7.43 (s, 2H, Ar-H), 7.51 (d, $J = 16.4$ Hz, 2H, *trans*-CH=CH-), 7.59 (s, 4H, Ar-H). IR (NaCl, thin film), ν_{max} (cm⁻¹): 3033 (m), 2956 (s), 2871 (m), 1513 (m), 1459 (s), 1382 (w), 1258 (w), 1212 (s), 965 (s), 849 (m). Anal. Calcd for C₂₁H₂₂O: C, 86.85; H, 7.64. Found: C, 85.72; H, 7.48.

Poly[(1-octyloxy-4-methyl-2,5-phenylenevinylene)-*alt*-(1,4-phenylenevinylene)] (2c) was synthesized in 30% yield by using the same procedure as for **2b**. ¹H NMR (CDCl₃, 400 MHz), δ : 0.87 (br, 3H, $-\text{CH}_2\text{CH}_3$), 1.22–1.61 (m, 6H, $-\text{CH}_2-$), 1.59 (br, 4H, $-\text{CH}_2-$), 1.85 (m, 2H, $-\text{CH}_2-$), 2.10 (s, 0.36H, Ar- CH_3 (*cis*-olefin fragment)), 2.39 (s, 2.64H, Ar- CH_3 (*trans*-olefin fragment)), 3.83 (m, 1.76H, $-\text{OCH}_2-$ (*trans*-olefin fragment)), 3.91 (m, 0.24 H, $-\text{OCH}_2-$ (*cis*-olefin fragment)), 7.13 (d, $J = 16.4$ Hz, 2H, *trans*-CH=CH-), 7.39 (s, 2H, Ar-H), 7.47 (d, $J = 16.4$ Hz, 2H, *trans*-CH=CH-), 7.55 (s, 4H, Ar-H). IR (NaCl, thin film), ν_{max} (cm⁻¹): 3033 (w), 2925 (s), 2856 (m), 1513 (w), 1382 (w), 1250 (m), 1212 (m), 1027 (s), 965 (s), 849 (w). Anal. Calcd for C₂₅H₃₀O: C, 86.66; H, 8.73. Found: C, 85.97; H, 8.71.

Synthesis of 3-Bromomethyl-4-hexyloxytoluene. To a suspension of 1-hexyloxy-4-methylbenzene (3.845 g, 20 mmol) and paraformaldehyde (0.615 g, 20.5 mmol) in acetic acid (10 mL) was added hydrogen bromide (30 wt % in AcOH, 4.09 mL, 20.5 mmol) via syringe. After the mixture was heated at 70–80 °C for 5 h, it was cooled to room temperature and poured onto ice/water (100 mL). The aqueous layer was extracted with four portions of hexanes (100 mL each). The combined organic layer was washed with water (four times, 20 mL each), and then dried over anhydrous MgSO₄. After removing the solvent on a rotatory evaporator, purification on column chromatography (silica gel, eluant hexanes) afforded 3-bromomethyl-4-hexyloxytoluene as a colorless oil (4.9 g, yield 86%). ¹H NMR (400 MHz, CDCl₃), δ : 0.90 (t, $J = 6.5$ Hz, 3H, $-\text{CH}_2\text{CH}_3$), 1.30–1.39 (m, 4H, $-\text{CH}_2-$), 1.46–1.56 (m, 2H, $-\text{CH}_2-$), 1.76–1.85 (m, 2H, $-\text{CH}_2-$), 2.26 (s, 3H, Ar- CH_3), 3.99 (t, $J = 6.4$ Hz, $-\text{OCH}_2-$), 4.54 (s, 2H, $-\text{CH}_2\text{Br}$), 6.75 (d, $J = 8.3$ Hz, 1H, Ar-*H*), 7.04 (d, $J = 8.3$ Hz, 1H, Ar-*H*), 7.12 (s, 1H, Ar-*H*). Anal. Calcd for C₁₄H₂₁BrO: C, 58.96; H, 7.42. Found: C, 58.68; H, 7.40.

Synthesis of Bis[2-(2-hexyloxy-5-methyl-1-phenyl)ethenyl]-1,4-benzene (7). A mixture of 3-bromomethyl-4-hexyloxytoluene (0.570 g, 2 mmol) and triethyl phosphite (0.40 g, 2.4 mmol) in a 25 mL flask was heated at 155–160 °C under an argon atmosphere for 5 h. The excess triethyl phosphite and byproducts were removed by vacuum (0.5 mmHg) at 100 °C for 0.5 h to give diethyl 2-hexyloxy-5-methylbenzylphosphonate (**6**) as a colorless liquid, which was then dissolved in 10 mL of anhydrous THF with terephthalaldehyde (**5**) (0.154 g, 1.15 mmol). To this solution was added potassium *tert*-butoxide (1 M in THF, 2.0 mL, 2 mmol) dropwise via a syringe over a period of 15 min. After addition, the reaction mixture was stirred for 4 h at room temperature. The clear solution was separated from precipitates via filtration. Following the removal of solvent, the product was purified by using column chromatography (silica gel, eluant: hexanes) to give pale yellow crystals (0.372 g, yield 72.8%, mp 90–92 °C). ¹H NMR (400 MHz, CDCl₃), δ : 0.95 (t, $J = 6.6$ Hz, 6H, $-\text{CH}_3$), 1.29–1.45 (m, 8H, $-\text{CH}_2-$), 1.52–1.60 (m, 4H, $-\text{CH}_2-$), 1.83–1.92 (m, 4H, $-\text{CH}_2-$), 2.35 (s, 6H, Ar- CH_3), 3.96 (t, $J = 6.5$ Hz, 0.28H, $-\text{OCH}_2-$ (*cis*-olefin fragment)), 4.03 (t, $J = 6.5$ Hz, 3.72H, $-\text{OCH}_2-$, *trans*-olefin fragment), 6.82 (d, $J = 8.2$ Hz, 2H, Ar-*H*), 7.04 (d, $J = 8.2$ Hz, 2H, Ar-*H*), 7.16 (d, $J = 16.4$ Hz, 2H, *trans*-CH=CH-), 7.43 (s, 2H, Ar-H), 7.50 (d, $J = 16.4$ Hz, 2H, *trans*-CH=CH-), 7.53 (s, 4 H, Ar-H). Anal. Calcd. C, 84.66; H, 9.08. Found: C, 84.42; H, 9.27.

LED Device Fabrication and Measurement. PEDOT/PSS (Bayer Co.) was spin-cast onto ITO glass (OFC Co.) to be used as an anode. The polymer solutions (20 mg/mL in chloroform) were filtered through 0.2 μm Millex-FGS Filters

(Millipore Co.), and were spin-cast onto ITO glass or dried PEDOT/ITO substrates under a nitrogen atmosphere. The polymer films were typically 75 nm thick. Calcium electrodes of 400 nm thickness were evaporated onto the polymer films at about 10^{-7} Torr, followed by a protective coating of aluminum. The devices were characterized using a system constructed in our laboratory described elsewhere.²⁰

Acknowledgment. Support of this work has been provided by AFOSR (Grant No. F49620-00-1-0090) and by NIH/NIGMS/MBRS/SCORE (Grant No. S06GM08247).

References and Notes

- (1) Burroughes, J. H.; Bradley, D. D. C.; Brown, A. R.; Marks, R. N.; Mackay, K.; Friend, R. H.; Burn, P. L.; Holmes, A. B. *Nature (London)* **1990**, *347*, 539–541.
- (2) For a recent review on electroluminescent conjugated polymers, see: Kraft, A.; Grimsdale, A. C.; Holmes, A. B. *Angew. Chem., Int. Ed.* **1998**, *37*, 402–428.
- (3) McGehee, M. D.; Heeger, A. J. *Adv. Mater.* **2000**, *12*, 1655–1668.
- (4) McQuade, D. T.; Pullen, A. E.; Swager, T. M. *Chem. Rev.* **2000**, *100*, 2537.
- (5) Skotheim, T. A.; Elsenbaumer, R. A.; Reynolds, J. R., Eds. *Handbook of Conducting Polymers*; Marcel Dekker: New York, 1998.
- (6) (a) Pang, Y.; Li, J.; Hu, B.; Karasz, F. E. *Macromolecules* **1999**, *32*, 3946–3950. (b) Davey, A. P.; Drury, A.; Maier, S.; Byrne, H. J.; Blau, W. J. *Synth. Met.* **1999**, *103*, 2478–2479. (c) Ohnishi, T.; Doi, S.; Tsuchida, Y.; Noguchi, T. *Photonic and Optoelectronic Polymers*; American Chemical Society: Washington, DC, 1997; pp 345–357. (d) Liao, L.; Pang, Y.; Ding, L.; Karasz, F. E. *Macromolecules*, **2001**, *34*, 6756–6760.
- (7) Some examples are as follows: (a) Li, J.; Pang, Y. *Macromolecules* **1998**, *31*, 5740–5745. (b) Xu, B.; Holdcroft, S. *Macromolecules* **1993**, *26*, 4457–4460.
- (8) Lawrence, N. J. The Wittig Reaction and Related Methods. In *Preparation of Alkenes: A Practical Approach*; Williams, J. M. J., Ed.; Oxford University Press: New York, 1996.
- (9) Lin-Vien, D.; Colthup, N. B.; Fateley, W. G.; Grasselli, J. G. *The Handbook of Infrared and Raman Characteristic Frequencies of Organic Molecules*; Academic: Boston, MA, 1991; Chapter 6.
- (10) Silverstein, R. M.; Bassler, G. C.; Morrill, T. C. *Spectrometric Identification of Organic Compounds*, 5th ed.; John Wiley & Sons: New York, 1991; pp 192, 193, 221.
- (11) Reference 10; Chapter 7.
- (12) The ϕ_{fl} value for **2** appeared to be dependent on the excitation wavelength used. When excited at 350 and 366 nm, for example, the solution of **2b** gave the ϕ_{fl} values of 0.85 and 0.71, respectively. Under the same condition, the solution of **1** (R = *n*-hexyl) gave the ϕ_{fl} values of 0.66 when excited at 366 nm. The ϕ_{fl} values listed in Table 1 are obtained by exciting the sample solution at 366 nm.
- (13) 1,4-Bis(2'-phenylethenyl)-2,5-dihexyloxybenzene^{6a} is the model chromophore for polymer **1**. Its UV-vis absorption shows $\lambda_{\text{max}} = 325$ and 388 nm in THF at room temperature.
- (14) Turro, N. J. *Modern Molecular Photochemistry*; University Science: Mill Valley, CA, 1991; Chapter 4.
- (15) Perkampus, H.-H. *UV-vis Spectroscopy and Its Applications*; Springer-Verlag: Berlin, 1992; Chapter 8.
- (16) Schäfer, E. P. *Dye Lasers*, 3rd ed.; Springer-Verlag: Berlin, 1990; p 18.
- (17) Liao, L.; Pang, Y. *J. Mater. Chem.* **2001**, *11*, 3078–3081.
- (18) Baigent, D. R.; Friend, R. H.; Lee, J. K.; Schrock, R. R. *Synth. Met.* **1995**, *71*, 2171–2172.
- (19) Liao, L.; Pang, Y.; Ding, L.; Karasz, F. E. *Macromolecules* **2001**, *34*, 7300–7305.
- (20) Hu, B.; Karasz, F. E. *Chem. Phys.* **1998**, *227*, 263–270.

MA012178R